

Study of the Photothermal Response of a Junction Vertical Parallel Silicon Solar Cell under a Multispectral Illumination

Gökhan ŞAHİN

Electric and Electronic Engineering Department, IĞDIR University, Iğdır 76000, Turkey
gokhan.sahin@igdir.edu.tr

Abstract- This study investigates the study of the photo thermal response of a junction vertical parallel silicon solar cell illuminated by a multispectral light for a constant modulated frequency. Solving the continuity equation for minority carriers in the base of the solar cell resulting in the terms of the heat equations in the presence of an optical source. The density of minority carriers in excess, the amplitude of the variation of temperature and the heat flux density were studied and analyzed for different angular pulses and junction recombination velocity. It also deals use of a new approach that involves parameter of the solar cell. Based on the normalized carrier's density, we calculate and plot the temperature and heat flux variation versus base depth, angular frequency, incidence angle and wavelength for different operating conditions.

Keywords- Vertical Parallel Junction Silicon Solar Cell; Temperature; Heat Flux

I. INTRODUCTION

The efficiency of a solar cell depends on among others on its intrinsic parameters. Therefore the knowledge of these parameters and control of associated technological processes highlighted below, are essential for any improvement of the conversion efficiency expected from the solar cell. Various characterization techniques have been implemented both in static frequency regime [1, 2] and in dynamic, i.e., the transient system [3, 4].

The objective of this paper is to extend the previously developed theory [5-9]. To study the effects of angular frequency (ω), incidence angle (θ), depth (z), junction recombination velocity (S_f); and the wavelength (λ) on the photovoltaic parameters of preferentially doped polysilicon solar cells.

II. THEORY

We consider a multi-crystalline junction vertical parallel silicon solar cell with n+-p structure in Fig. 1. Since the base has a greater contribution to photo conversion, the one-dimensional analysis will be focused only on this region using the Quasi-Neutral Base assumption.

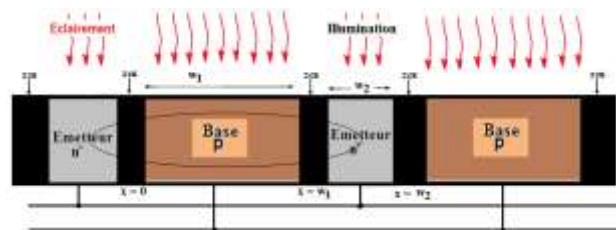


Fig. 1 Vertical parallel junction silicon solar cell

We present in Fig. 2 a unit cell of a vertical junction's silicon solar cell under various wavelengths. H is the base width; θ is the illumination incidence angle and x is the depth in the base.

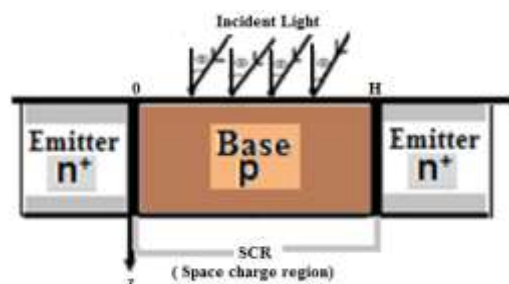


Fig. 2 A unit cell of a vertical parallel junction silicon solar cell

When the silicon solar cell is illuminated with a frequency modulated monochromatic light, the diffusion equation about excess minority carriers (electrons) density photogenerated in the base region can be written as [10-14]:

$$D(\omega) \cdot \frac{\partial^2 \delta(x, \theta, t)}{\partial x^2} - \frac{\delta(x, \theta, t)}{\tau} = -G(z, \theta, t) + \frac{\partial \delta(x, \theta, t)}{\partial t} \quad (1)$$

$D(\omega)$ [15] and τ are, respectively, the excess minority carrier diffusion constant and lifetime.

The excess minority carrier's density is written as (2):

$$\delta(x, t) = \delta(x) \exp(-j\omega t) \quad (2)$$

and

$$G(z, \theta, \lambda, t) = g(z, \theta, \lambda) \exp(-j\omega t) \quad (3)$$

where

$$g(z, \theta, \lambda) = \alpha(\lambda)(1 - R(\lambda)) \cdot \phi(\lambda) \cdot \exp(-\alpha(\lambda) \cdot z) \cdot \cos(\theta) \quad (4)$$

x is the base depth along x -axis, ω is the angular frequency, θ is the incidence angle, z the base depth according to the vertical axis; Sf is the junction recombination velocity, and λ the illumination wavelength.

If we replace equation (2) into equation (1), the temporary part is eliminated, and we obtain:

$$\frac{\partial^2 \delta(x)}{\partial x^2} - \frac{\delta(x, \theta, t)}{L(\omega)^2} = -\frac{g(z, \theta)}{D(\omega)} \quad (5)$$

The solution of this equation is written as:

$$\delta(x, \omega, \theta, z, Sf, \lambda) = A \cosh\left(\frac{x}{L(\omega)}\right) + B \sinh\left(\frac{x}{L(\omega)}\right) + \frac{L(\omega)^2}{D(\omega)} \cdot \alpha(\lambda)(1 - R(\lambda)) \cdot \phi(\lambda) \cdot \exp(\alpha(\lambda) \cdot z) \cdot \cos(\theta) \quad (6)$$

Coefficients A and B determine through the following boundary conditions [15]:

- at emitter-base junction ($x = 0$):

$$D(\omega) \cdot \left. \frac{\partial \delta(x, \omega, \theta)}{\partial x} \right|_{x=0} = Sf \cdot \delta(x, \omega, \theta) \Big|_{x=0} \quad (7)$$

- at the middle of the base ($x = H/2$) [16]:

$$D(\omega) \cdot \left. \frac{\partial \delta(x, \omega, \theta)}{\partial x} \right|_{x=\frac{H}{2}} = 0 \quad (8)$$

Sf is the excess minority carrier recombination velocity at each junction [17].

When a solar cell is subjected to a constant monochromatic optical excitation frequency modulated, minority charge carriers (electrons) are generated in the solar cell. It follows a temperature rise of the solar cell due to the thermalization (energy photons or less than the gap), the movement of carriers (mainly diffusion in the base) [18]. This rise in temperature about the equilibrium temperature of the material is the result of a heat-flux, which propagates through the solar cell. For a small change in temperature from the initial temperature T_0 , the heat flux in the solar cell can be described by the equation [18-20].

$$a \cdot \frac{\partial^2 \Delta T(x, t)}{\partial x^2} + \frac{G(z, t)}{\rho \cdot c} = \frac{\partial \Delta T(x, t)}{\partial t} \quad (9)$$

With the thermal diffusivity of material, ρ the density and c specific heat, the terms $\Delta T(x, t)$ and $G(z, t)$ represent the temperature variation respectively compared to the initial temperature T_0 and the thermal rate of generation according to time [18, 21].

$$\Delta T(x, t) = \Delta T(x) \cdot e^{i\omega t} \quad (10)$$

$$G(z, t) = G(z) \cdot e^{i\omega t} \quad (11)$$

$\Delta T(x)$ and $G(z)$ are the space components of the temperature and the thermal rate of generation.

The term $e^{i\omega t}$ represents the temporal component of the temperature and the heat rate production. This temporal component has the same pulsation $\omega=2\cdot\pi\cdot f$ as the incidence optical beam at every moment.

The equation (12) can be still written:

$$\frac{\partial^2 \Delta T(x, \omega, \theta, \lambda)}{\partial x^2} - \sigma(\omega)^2 \Delta T(x, \omega, \theta, \lambda) = -\frac{G(x, \omega, \theta, \lambda)}{k} \quad (12)$$

where

$$G(x, \omega, \theta, \lambda) = \alpha(\lambda) \cdot \phi(\lambda) \cdot (1 - R(\lambda)) \cdot \Delta E \cdot \cos(\theta) \cdot e^{-\alpha(\lambda) \cdot z} \cdot e^{-i\omega x} + \frac{E_g \cdot \delta(x, \omega, \theta, \lambda)}{\tau} \cdot \cos(\theta) \quad (13)$$

$\sigma(\omega) = \left(\frac{i \cdot \omega}{a}\right)^{1/2}$ is the thermal coefficient of diffusion process complexes k is thermal conductivity. $\Delta E = (h\nu - E_g)$ is the energy variation, E_g is the gap silicon energy.

$$\frac{\partial^2 \Delta T(x)}{\partial x^2} - \sigma(\omega)^2 \Delta T(x) = -\frac{G(z)}{k} \quad (14)$$

where

$$\Delta T_1(x, \omega) = \frac{E_g}{k\tau(\sigma(\omega)^2 - L(\omega)^{-2})} \left\{ \frac{A(\omega) \cdot \cosh\left(\frac{x}{L(\omega)}\right) + B(\omega) \cdot \sinh\left(\frac{x}{L(\omega)}\right)}{\right\} + \frac{\alpha(\lambda) \cdot \phi(\lambda) \cdot (1 - R(\lambda))}{k \cdot (\sigma(\omega)^2 - \alpha(\lambda)^2)} \left\{ \Delta E + \frac{E_g L(\omega)^2}{D(\omega) \cdot \tau \cdot (1 - \alpha(\lambda)^2 L(\omega)^2)} \right\} \cdot e^{-\alpha(\lambda) \cdot z} \quad (15)$$

We can write

$$\frac{\partial^2 \Delta T(x)}{\partial x^2} - \sigma(\omega)^2 \cdot \Delta T(x) = 0 \quad (16)$$

where

$$\Delta T_2(x, \omega, \theta, \lambda) = C(\omega) \cdot \cosh(\sigma(\omega) \cdot x) + D(\omega) \cdot \sinh(\sigma(\omega) \cdot x) \quad (17)$$

The general solution is given by the following expression:

$$\Delta T(x, \omega, \theta, \lambda) = C(\omega) \cdot \cosh\left(\frac{x}{L(\omega)}\right) + D(\omega) \cdot \sinh\left(\frac{x}{L(\omega)}\right) + \frac{E_g}{k \cdot \tau \cdot (1 - \alpha(\lambda)^2 \cdot L(\omega)^2)} \left\{ \frac{A(\omega) \cdot \cosh\left(\frac{x}{L(\omega)}\right) + B(\omega) \cdot \sinh\left(\frac{x}{L(\omega)}\right)}{\right\} + \frac{\alpha(\lambda) \cdot \phi(\lambda) \cdot (1 - R(\lambda))}{k \cdot (\sigma(\omega)^2 - \alpha(\lambda)^2)} \left\{ \Delta E + \frac{E_g \cdot L(\omega)^2}{D(\omega) \cdot \tau \cdot (1 - \alpha(\lambda)^2 \cdot L(\omega)^2)} \right\} \cdot e^{-\alpha(\lambda) \cdot z} \quad (18)$$

Coefficients C and D are determined through the following boundary conditions [22, 23]:

- at emitter-base junction ($x = 0$):

$$\frac{\partial \Delta T(x, \omega, \theta, \lambda)}{\partial x} \Big|_{x=0} = Sf(p) \cdot \frac{E_g \delta(x=0, \omega)}{k} \quad (19)$$

- at the middle of the base ($x = H/2$):

$$\frac{\partial \Delta T(x, \omega, \theta, \lambda)}{\partial x} \Big|_{x=\frac{H}{2}} = 0 \quad (20)$$

In the continuation of our work, assumptions, and operating conditions remain unchanged; we will only consider the phenomenological variables and modules power of the solar cell. The heating of the solar cell that is to say the variation in the temperature of the solar cell is directly related to the heat flux density. This heat flux density expresses in [24].

$$\phi(x, \omega, \theta, \lambda) = -k \cdot \frac{\partial \Delta T(x, \omega, \theta, \lambda)}{\partial x} \quad (21)$$

After calculation, all these sizes thus determined are complex and can be put in the form of a complex.

III. RESULTS AND DISCUSSION

The output power of a solar module is affected by the temperature of the solar cells. In Crystalline PV (photovoltaic) module, effects can be as much as 0.5% for every one-degree variation in temperature. It is useful to understand the effect of the spectrum of the incident light and temperature on the solar cell and module performance, to estimate their performance under various climate conditions. We are now studying the variations of the temperature and heat flux density in the database according to the following depth x .

A. Effect of Frequency

We represented on Fig. 3(a) and 3(b) the temperature and heat flux variation within the polysilicon solar cell under monochromatic illumination versus the depth according to horizontal (x) for various frequencies.

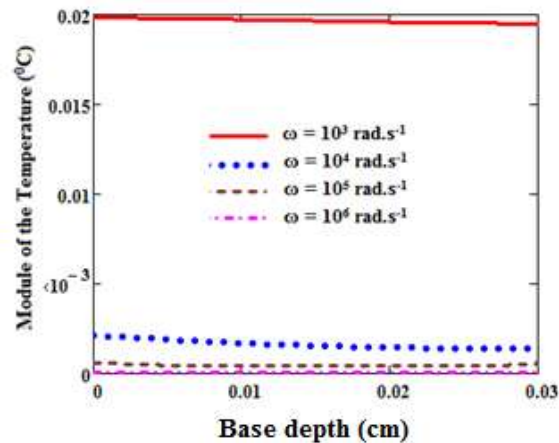


Fig. 3(a) Modules of the variation of the temperature versus base depth for various modulation frequencies: $S_f = 2.10^2 \text{ cm/s}$, $H = 0.03 \text{ cm}$, $L_o = 0.02 \text{ cm}$, $D_o = 26 \text{ cm}^2/\text{s}$, $\lambda = 50 \mu\text{m}$, $z = 0.0001 \text{ cm}$, $\theta = 48.2^\circ$

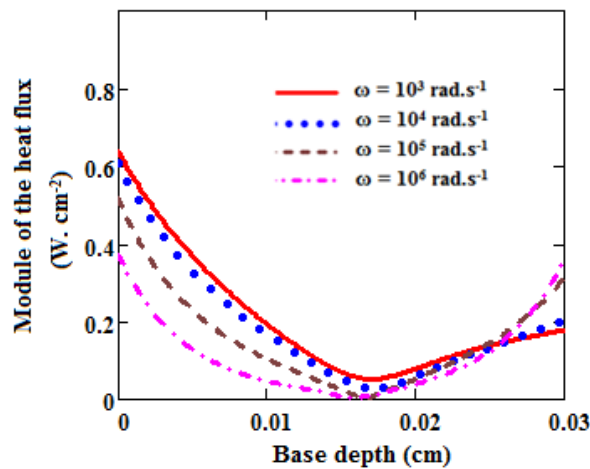


Fig. 3(b) Modules of the variation of the heat flux versus the base depth for various modulation frequencies

$$S_f = 2.10^2 \text{ cm/s}, H = 0.03 \text{ cm}, L_o = 0.02 \text{ cm}, D_o = 26 \text{ cm}^2/\text{s}, \lambda = 50 \mu\text{m}, z = 0.0001 \text{ cm}, \theta = 48.2^\circ$$

Considering one curve of the temperature change within the base, we notice that it decreases until a minimum ($x=H/2$). When depth is higher than $H/2$, the temperature variation increases until the depth limit ($x = H$). Thus, we note three zones on the curve representative the temperature change within the polysilicon solar cell versus the depth according to horizontal x :

Zone 1 ($0 \leq x < H/2$): where the gradient of the temperature difference is negative. What defames a significant passage of electrons a thus translating of a high-temperature flow with the junction emitter-base.

Zone 2 ($x = H/2$): the gradient of the temperature variation is null translating the static effect of the minority carriers in the base. This absence of movement of minority carriers in the base gives rise to a temperature minimum noted on the figure.

Zone 3 ($H/2 < x \leq H$): where the gradient of the temperature variation the base is active translating a significant passage of minority carriers thus an increase in heat, due to the diffusion and the shocks, the junction emitter-bases.

Indeed the generation being higher on the junctions, we note there is a greater presence of minority carriers. We note that the diffusion of these carriers occurs on this sites. Then we can provide that there are more shocks involving the temperature

rise. More than one enters depth x ; the material becomes less conducting giving fewer shocks from where temperature reduction.

This figure shows that the temperature variation is greater in the vicinity of the junction; indeed, given the thermalization and diffusion processes in the solar cell, the average temperature of the solar cell will increase, but this increase will be more significant to the junction since the flow of carriers there will be the greatest. The profile of the heat flux density (Fig. 3b) confirmed this analysis.

We can predict that the closer a short circuit operation, plus the temperature change will be necessary for the base but even more so in the vicinity of the junction. When the operating frequency increases, there is not only little generation but also, less moving carriers, since the diffusion coefficient decreases sharply with this modulation frequency: a decrease can thus be observed in the variation of the temperature.

B. Effect of Incidence Angle

We represented on Fig. 4(a) and Fig. 4(b) are the temperature and heat flow variation within the polysilicon solar cell under monochromatic illumination versus the depth according to horizontal x for various incidence angles.

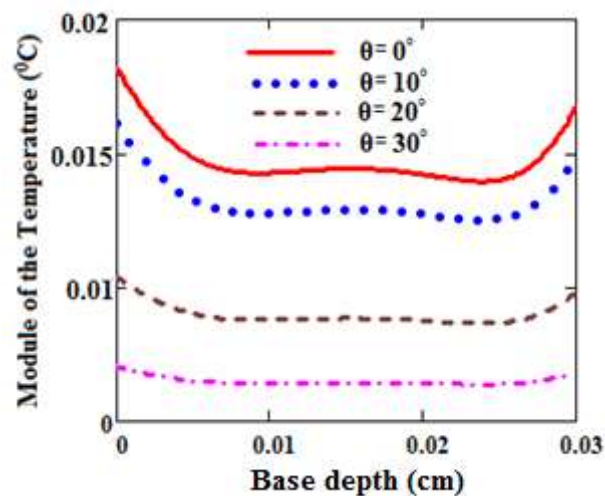


Fig. 4(a) Modules of the variation of the temperature versus the base depth for various different incidence angles:

$$S_f = 2 \cdot 10^2 \text{ cm/s}, H = 0.03 \text{ cm}, L_o = 0.02 \text{ cm}, D_o = 26 \text{ cm}^2/\text{s}, \lambda = 50 \mu\text{m}, z = 0.0001 \text{ cm}, \omega = 10^5 \text{ rad/s}$$

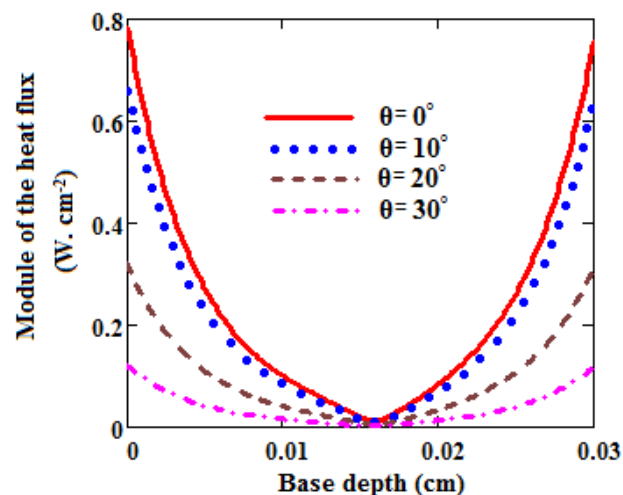


Fig. 4(b) Modules of the variation of the heat flux versus the base depth for various different incidence angles:

$$S_f = 2 \cdot 10^2 \text{ cm/s}, H = 0.03 \text{ cm}, L_o = 0.02 \text{ cm}, D_o = 26 \text{ cm}^2/\text{s}, \lambda = 50 \mu\text{m}, z = 0.0001 \text{ cm}, \omega = 10^5 \text{ rad/s}$$

We observe Fig. 4 (a) the temperature variations are greater in the vicinity of junctions; when the incidence angles are increases. The light intensity decreases so that the carrier density decreases at the same pace. This decline in the carrier density in the material causes a reduction in the heating of the solar cell: we can well see that the heat flux density is directly related to the heating profile in Fig. 4(b).

C. Effect of Wavelength

We represented on Fig. 5(a), Fig. 5(b), Fig. 6(a) and Fig. 6 (b) the temperature and heat flux variation within the polysilicon solar cells under monochromatic illumination versus the depth according to horizontal x for various wavelengths.

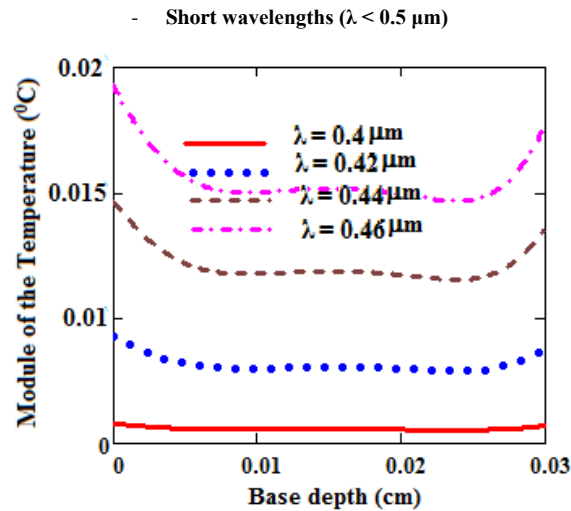


Fig. 5(a) Modules of the variation of the temperature versus the base depth for various short wavelengths λ

$$H = 0.03\text{cm}, L_o = 0.02\text{cm}, D_o = 26\text{cm}^2/\text{s}, z = 0.0001\text{cm}, \theta = 48.2^\circ, z = 0.0001\text{cm}, \omega = 10^5\text{rad/s}$$

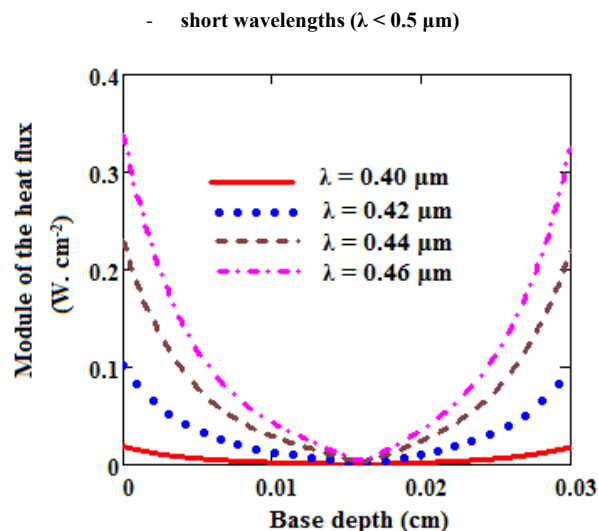


Fig. 5(b) Modules of the change of the heat flux versus the base depth for various short wavelengths λ

$$H = 0.03\text{cm}, L_o = 0.02\text{cm}, D_o = 26\text{cm}^2/\text{s}, z = 0.0001\text{cm}, \theta = 48.2^\circ, z = 0.0001\text{cm}, \omega = 10^5\text{rad/s}$$

For the short wavelengths [0.4 μm ; 0.46 μm], the wavelength increases and the amplitudes of the temperature, heat flux increase too. Contrary for the long wavelengths [0.78 μm ; 0.98 μm]; in other words, if the wavelength increases, the amplitudes of the temperature and heat flux are decreased. For this type of polysilicon solar cell, the long wavelengths should have limited by the optical and electric properties material. This can predict the range wavelength where it is necessary to work to have a better output. In the area of short wavelengths, the energy increases with the wavelength; this means that in this range, the energy carried by the excitement increases is to say that the energy imparted to the solar cell. The heating of the solar cell will, therefore, increase with the wavelength in the range of short wavelengths.

With long wavelengths, the energy decreases with the wavelength, and there is a decline in the transmitted power and thus the heating with the wavelength.

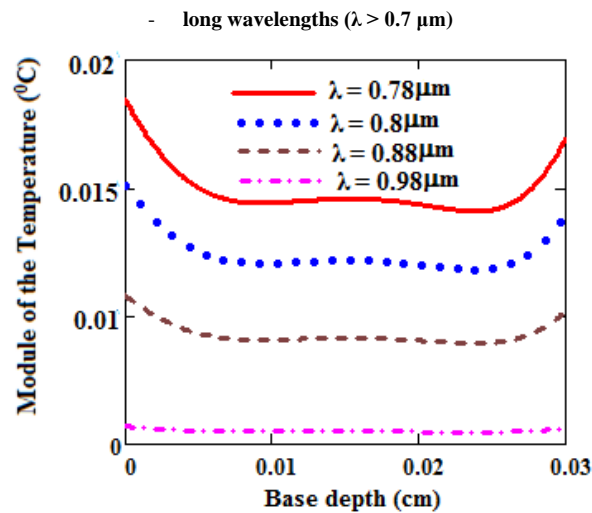


Fig. 6(a) Modules of the variation of the temperature versus the base depth for various different long wavelengths

$$\lambda: H = 0.03\text{cm}, L_o = 0.02\text{cm}, D_o = 26\text{cm}^2/\text{s}, z = 0.0001\text{cm}, \theta = 48.2^\circ, z = 0.0001\text{cm}, \omega = 10^5\text{rad/s}$$

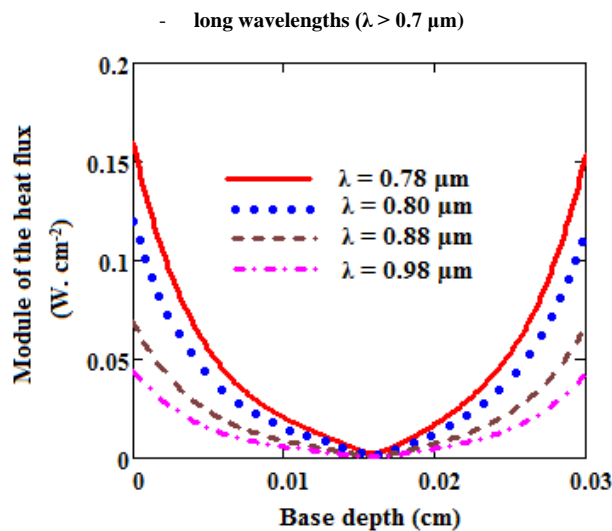


Fig. 6(b) Modules of the variation of the heat flux versus the base depth for various long wavelengths λ

$$H = 0.03\text{cm}, L_o = 0.02\text{cm}, D_o = 26\text{cm}^2/\text{s}, z = 0.0001\text{cm}, \theta = 48.2^\circ, z = 0.0001\text{cm}, \omega = 10^5\text{rad/s}$$

IV. CONCLUSIONS

The formalism proposed in this study considered a solar cell is operating under a multispectral illumination with a modulated frequency. Through the use of phenomenological parameters such as recombination velocities at the junction and the thermal behavior of the solar cell, we analyzed and studied the density of minority charge carriers, the temperature amplitude and the density of heat flux. We found out that any increase in temperature results in a decrease of electrical power delivered by the base of the solar cell. For values of $T < 10^4$ rad/s, the density of minority carriers in excess, the variation of temperature and the heat flux density remain almost constant; such parameters are weakly influenced by the angle of the signal pulse: it is thus a situation of a static regime. For values of $T > 10^4$ rad/s, the density of minority carriers in excess, the variation of temperature and the heat flux density decrease when the pulse angle of the signal increases: it regards a case of purely frequency regime, and these parameters are highly dependent on the pulse angle. The variation of the temperature and heat flux as a function of the depth x have been studied on the various parameters such as the angular frequency, the incident angles, and wavelength. The study shows that the temperature and thus the heat flux is higher in the vicinity of the junction decreasing depth in the base.

The temperature and heat flux decreases with increasing angular frequency, incidence angle, according to the range of wavelengths while it has the opposite effect with the range of short wavelengths.

REFERENCES

- [1] F. I. Barro, E. Nanema, A. Wereme, F. Zougmore, and G. Sissoko, "Recombination parameters measurement in silicon Double sided

- surface field solar cell,” *J. Des. Sci.*, vol. 1(1), pp. 76-80, 2001.
- [2] O. H. Lemrabott, I. Ly, A. S. Maiga, A. Wereme, F. I. Barro, and G. Sissoko, “Bulk and surface recombination parameters measurement in silicon double sided solar cell under constant monochromatic illumination,” *J. of Sci.*, vol. 8(1), pp. 44-50, 2008.
- [3] A. Dieng, O.H. Lemrabott, A.S. Maiga, A. Diao, and G. Sissoko, “Impedance spectroscopy method applied to electrical parameters determination on bifacial silicon solar cell under magnetic field,” *J. of Sci.*, vol. 7(3), pp. 48-52, 2007.
- [4] F. I. Barro, E. Nanema, F. Zougmore, A. Wereme, A. Ndiaye, and G. Sissoko, “Transient study of double sided silicon solar cell under constant white bias light: Determination of recombination parameters,” *J. Des. Sci.*, vol. 3(1), pp. 10-14, 2003.
- [5] N. Dieme, “Study of the performance of a parallel vertical junction Silicon solar cell under thermal influence,” *Asian Academic Research Journal of Multidisciplinary*, vol. 2, pp. 2319-280, 2015.
- [6] R Pässler, “Semi-empirical descriptions of temperature dependences of band gaps in semiconductors,” *Phys. Stat. Sol.*, vol. 236, pp. 710-728, 2003.
- [7] Turgut G, Kocyigit A, and Sonmez E, “Influences of Pr and Ta doping concentration on the characteristic features of FTO thin film deposited by spray pyrolysis,” *Chinese Physics B*, vol. 24, iss. 10, pp. 414-422, 2015.
- [8] M. Sane, M. Zoungrana, H. L. Diallo, G. Sahin, N. Thiam, M. Ndiaye, M. Dieng, and G. Sissoko, “Influence of Incidence Angle on the Electrical Parameters of a vertical Silicon Solar Cell under Frequency Modulation,” *International Journal of Inventive Engineering and Sciences (IJIES)*, vol. 1, pp. 2319-9598, 2013.
- [9] R. Topkaya, H. Güngüneş, Ş. Eryiğit, Sagar E. Shirsath, A. Yıldız, and A. Baykal, “Effect of bimetallic (Ni and Co) substitution on magnetic properties of MnFe₂O₄ nano particles,” *Ceramics International*, vol. 42, iss. 12, pp. 13773-13782, September 2016.
- [10] N. Honma and C. Munakata, “Sample thickness dependence of minority carrier Lifetimes Measured using an ac photovoltaic Method,” *Japanese Journal of Applied Physics*, vol. 26, no. 12, pp. 233-236, December 1987.
- [11] N. Honma, C. Munakata, and H. Shimizu, “Calibration of minority carrier lifetimes measured with an ac photovoltaic method,” *Japanese Journal of Applied Physics*, vol. 27, no. 7, pp. 1322-1326, July 1988.
- [12] A. Mandelis, “Coupled ac photocurrent and photothermal reflectance response theory of semiconducting p-n junctions,” *J. Appl. Phys.*, vol. 66(11), pp. 5572-5583, 1 December 1989.
- [13] A. Dieng, I. Zerbo, M. Wade, A. S. Maiga, and G. Sissoko, “Three-dimensional study of a polycrystalline silicon solar cell: the influence of the applied magnetic field on the electrical parameters,” *Semicond. Sci. Technol.*, vol. 26, no. 9, pp. 95023-95031, August 2011.
- [14] G Sahin, “Effect of wavelength on the electrical parameters of a vertical parallel junction silicon solar cell illuminated by its rear side in frequency domain,” *Results in Physics*, vol. 6, pp. 107-111, March 2016.
- [15] A. Gover and P. Stella, “Vertical Multijunction Solar-Cell One-Dimensional Analysis,” *IEEE Transactions on Electron Devices*, vol. 21, iss. 6, pp. 351-356, June 1974.
- [16] M. Bashahuand and A. Habyarimana, “Review and test of methods for determination of the solar cell series resistance,” *Renewable Energy*, vol. 6(2), pp. 127-138, 1995.
- [17] E. H. Ndiaye, G. Sahin, M. Dieng, A. Thiam, H. L. Diallo, M. Ndiaye, and G. Sissoko, “Study of the Intrinsic Recombination Velocity at the Junction of Silicon Solar under Frequency Modulation and Irradiation,” *Journal of Applied Mathematics and Physics*, vol. 3, pp. 1522-1535, November 2015.
- [18] A. Mandelis, “Coupled ac photocurrent and photothermal reflectance response theory of semiconducting p-n junctions: I,” *J. Appl. Phys.*, vol. 66(11), pp. 5572-5583, 1989.
- [19] V. S. Vikhrenko, *Heat Transfer – Engineering Applications*, ISBN 978-953-307-361-3, 3rd ed., 412 pages, Publisher: InTech, DOI: 10.5772/2434, December 2011.
- [20] M. Kaviany, *Essentials of Heat Transfer: Principles, Materials, and Applications*, 1st ed., 712 pages, Cambridge University Press, 2011.
- [21] A. Thiam, M. Zoungrana, H. Ly Diallo, A. Diao, N. Thiam, S. Gueye, M.M. Deme, M. Sarr, and G. Sissoko, “Influence of Incident Illumination Angle on Capacitance of a Silicon Solar Cell under Frequency Modulation,” *Res. J. Appl. Sci. Eng. Technol.*, vol. 5(04), pp. 1123-1128, 2012.
- [22] H. L. Diallo, A. Se ïlou Maiga, A. Wereme, and G. Sissoko, “New approach of both junction and back surface recombination velocities in a 3D modelling study of a polycrystalline silicon solar cell,” *The European Physical Journal Applied Physics*, vol. 42, iss. 03, pp. 203-211, June 2008.
- [23] H. L. Diallo, B. Dieng, I. Ly, and M. M. Dione, “Determination of the Recombination and Electrical Parameters of a Vertical Multijunction Silicon Solar Cell,” *Res. J. Appl. Sci. Eng. Technol.*, vol. 4(16), pp. 2626-2631, 2012.
- [24] Y. Gillet and C. Bissieux, “Diffusion harmonique de la chaleur appliquée au contrôle non destructif par méthodes photothermiques,” *Int. J. Therm. Sci.*, vol. 38, iss. 6, pp. 530-540, 1999.